Environ Geol
DOI 10.1007/s00254-007-0675-0

ORIGINAL ARTICLE

Bridging the gap between laboratory measurements and field estimations of silicate weathering using simple calculations

Jiwchar Ganor · Peng Lu · Zuoping Zheng · Chen Zhu

Received: 15 October 2006 / Accepted: 30 January 2007

Abstract Weathering rates of silicate minerals observed in the laboratory are in general up to five orders of magnitude higher than those inferred from field studies. Simple calculations show that even if the field conditions were fully simulated in standard laboratory experiments, it would be impossible to measure the slow rates of mineral dissolution that are observed in the field. As it is not possible to measure the dissolution rates under typical field conditions, one should extrapolate the available data to the field conditions. To do this, a rate law for the dissolution of plagioclase in the field was formulated by combining the far from equilibrium dissolution rate of weathered natural oligoclase at 25°C with the effect of deviation from equilibrium on dissolution rate of fresh albite at 80°C. In contrast to the common view that laboratory experiments predict dissolution rates that are faster than those in the field, the simulation based on this rate law indicates that laboratory dissolution experiments actually predict slower rates than those observed in the field. This discrepancy is explained by the effect of precipitation of secondary minerals on the degree of saturation of the primary minerals and therefore on their dissolution rate. Indeed, adding kaolinite precipitation to the simulation significantly enhances the dissolution rate of the plagioclase. Moreover, a strong coupling between oligoclase dissolution and kaolinite precipitation was observed in the simulation. We suggest that such a coupling must exist in the field as well. Therefore, any attempt to predict the dissolution rate in the field requires knowledge of the rate of the secondary mineral precipitation.

Keywords Aqueous geochemistry · Ground water · Waste water

J. Ganor (✉)
Department of Geological and Environmental Sciences,
Ben-Gurion University of the Negev, P. O. Box 653,
Beer-Sheva 84105, Israel
e-mail: ganor@bgu.ac.il
URL: http://www.bgu.ac.il/geol/ganor/

P. Lu · Z. Zheng · C. Zhu
Department of Geological Sciences, Indiana University,
1001 East 10th Street, Bloomington, IN 47405-1405, USA

Introduction

Quantification and understanding of low-temperature silicate dissolution and precipitation reactions have important implications for many environmental questions, including the neutralization of acid precipitation, the relationship between silicate weathering and global climate over geological timescales (e.g., Berner 1992), the balance of macronutrients such as K and Ca in forests (Huntington et al. 2000), the composition of ground water and surface water, and global geochemical cycles (Lasaga et al. 1994). Therefore, numerous laboratory experiments and field-based studies have been conducted to quantify the dissolution rates of silicate minerals. A comparison of the results of these two approaches shows that weathering rates of silicate minerals observed in the laboratory are in general several orders of magnitude higher than those inferred from field studies (Schnoor 1990; Stumm 1992; van Grinsven and van Riemsdijk 1992; Anbeek 1993; Casey et al. 1993; Velbel 1993;

Blum and Stillings 1995; White and Brantley 1995; Drever 2003; White and Brantley 2003; Zhu et al. 2004; Zhu 2005). The many differences between experimental conditions in the laboratory and natural conditions in the field were thoroughly discussed in previous studies (e.g., White and Brantley 2003, and references therein). In short, these differences include: efficiency of solution/mineral contact, duration of weathering, aging of surfaces, presence and depth of defects and etch pits, formation of leached layers, surface coatings, degree of undersaturation, and solution chemistry in micro-pores. Note that microorganism activities actually accelerate the weathering rates, which exasperate the discrepancy between field and lab rates. Despite the thorough discussion of the differences between the environmental conditions in the field and in laboratory experimental settings, there has been no successful attempt to fully simulate the field environmental conditions in laboratory experiments, and consequently to measure the slow rates observed in the field in these experiments.

A possible explanation is that the duration of chemical weathering in the field is too long to be simulated in the laboratory (Casey et al. 1993). Taylor and Blum (1995) showed that weathering rates at different field-sites varied by a few orders of magnitude, and were found to decrease with soil age. The effect of duration of weathering on its rate was studied by White and Brantley (2003), who divided the rate controlling properties to intrinsic factors, which are physical and chemical properties of the mineral and its surfaces (e.g., surface aging and coating) and extrinsic factors, which are environmental conditions external to the dissolving mineral (e.g., degree of saturation). Adopting this approach, it seems that the slow dissolution rates that are typically observed in the field should be observable in laboratory experiments in which highly weathered natural samples would be dissolved under environmental conditions that are similar to those in the field.

The major aim of the present paper is to explore three aspects of the gap between laboratory measurements and field estimations of weathering using simple calculations: (1) to determine whether or not it is possible to measure the slow rates observed in the field using conventional laboratory experiments; (2) to show that although the dissolution rate in each of the laboratory experiments is faster, the dissolution rate extrapolated to field conditions should be even slower than what is actually observed in the field; and (3) to demonstrate that the rate of dissolution of the primary minerals is strongly coupled to the rate of precipitation of secondary minerals.

Discussion

It is not possible to measure field dissolution rates of silicates using standard laboratory experiments

Field-based dissolution rates are usually estimated by mass balance approaches in soil profiles and watersheds (see recent review in White and Brantley 2003; Bricker et al. 2004). The dissolution rate of Na-rich plagioclase (albite to labradorite) in these studies ranges between 4×10^{-17} and 2×10^{-13} mol m^{-2} s^{-1} (White and Brantley 2003). This wide range of rates reflects both differences in environmental conditions and in the reactivity of the mineral surfaces. As a case study, we will evaluate the possibility of conducting laboratory experiments simulating the dissolution of plagioclase in the Panola regolith (Georgia Piedmont Province, USA), which was estimated in the field to be 2×10^{-16} mol m^{-2} s^{-1} (White and Brantley 2003). We choose this case study for the following reasons: (1) plagioclase is a common mineral and its dissolution rate has been investigated in many field and laboratory studies; (2) the environmental conditions at this site are well characterized; (3) far from equilibrium dissolution rates of natural samples from the Panola regolith have been measured in laboratory experiments (White and Brantley 2003); and (4) the estimated in situ plagioclase dissolution rate in the Panola regolith is in agreement with other field studies and does not represent an extreme or unusual value. As in many other natural systems, the dissolution of silicates in the Panola regolith is incongruent, and occurs under near equilibrium conditions. The average Gibbs free energy of reaction with respect to albite dissolution (which serves as a proxy to the Na-rich oligoclase) in the Panola ground water is –10.9 kJ mol^{-1} (White and Brantley 2003).

In order to check if the field-based dissolution rate can be measured in laboratory experiments, we calculated the expected outcome of hypothetical experiments conducted under conditions similar to those in the Panola ground water using standard experimental conditions. The following common parameters were used in all the calculations: The dissolved mineral is an oligoclase ($Na_{0.77}Ca_{0.23}Al_{1.23}Si_{2.77}O_8$ [White et al. 2002]) with a specific surface area of 1 m^2 g^{-1} (White and Brantley 2003). The solution has the same composition as average pore water at a depth of 3 m from saprolite of the Panola regolith (Table 1, data after White et al. 2002). This pore water is oversaturated with respect to pyrophyllite ($Al_2Si_4O_{10}(OH)_2$) and kaolinite ($Al_2Si_2O_5(OH)_4$) and to a lesser extent with respect to a few other minerals (Table 2) (White et al.

Table 1 Chemical concentrations (μmol l^{-1}) of major elements in average pore water from a depth of 3 m in Panola watershed (Data from White et al. 2002, Table 3)

pH	Na	K	Ca	Mg	Al	SiO_2	Alkalinity	Cl	NO_3	SO_4
5.37	206	17.7	12.5	56.4	2.3	189	25.4	319	2.8	1.6

Table 2 Oversaturated minerals determined from pore water chemistry at Panola watershed (Table 1)

Phase	SI	Formula
Pyrophyllite	7.03	$Al_2Si_4O_{10}(OH)_2$
Kaolinite	5.2	$Al_2Si_2O_5(OH)_4$
Muscovite	4.1	$KAl_3Si_3O_{10}(OH)_2$
Halloysite	1.93	$Al_2Si_2O_5(OH)_4$
Diaspore	1.58	AlO(OH)
Quartz	1.14	SiO_2
Cristobalite	0.72	SiO_2
Chalcedony	0.66	SiO_2
Leonhardite	0.59	$Ca_2Al_4Si_8O_{24}{\cdot}7H_2O$
SiO_2 (a)	0.15	SiO_2

SI saturation index. Calculations were conducted using PHREEQC software with MINETQ database

2001). As kaolinite is the major secondary mineral in the regolith (White et al. 2001), we will assume that it would be precipitated during the dissolution of the oligoclase. To keep the calculations simple, we assume that aluminum concentration remains constant due to a balance between oligoclase dissolution and kaolinite precipitation (e.g., White et al. 2001). Adopting an alternative assumption that the solution is constantly in equilibrium with respect to kaolinite, would not influence the results of the calculations because aluminum concentrations are very low. We further assume that both oligoclase is dissolved and kaolinite is precipitated stoichiometrically, and therefore the reaction may be described by:

$$\begin{aligned} &Na_{0.77}Ca_{0.23}Al_{1.23}Si_{2.77}O_8 + 1.23H^+ + 3.695H_2O \\ &\quad \rightarrow 0.615Al_2Si_2O_5(OH)_4 + 1.54H_4SiO_4 + 0.23Ca^{2+} \\ &\qquad + 0.77Na^+ \end{aligned} \tag{1}$$

The significance of the stoichiometry of Eq. (1) will be further discussed later. If the dissolution rates of oligoclase in the experiment were the same as was estimated in the field (2×10^{-16} mol m^{-2} s^{-1} [White and Brantley 2003]), the net release rate of Si would be 3.1×10^{-16} mol m^{-2} s^{-1}, and that of Na 1.54×10^{-16} mol m^{-2} s^{-1}. As the initial concentration of both elements in the solution is about the same (Table 1), and the release rate of Si is faster, it would be easier to detect changes in the concentration of Si compared to Na. Therefore, only the change of Si concentration will be discussed below. If the uncertainty in the determination of Si concentration in solution is ±2%, an increase of 2.8% between two measurements would be detectable, assuming that the two measurements are independent of each other.

The many different experimental designs (e.g., pH-stat, stirred batch, fluidized bed, stirred flow-through and column) that are available to determine dissolution rates may be classified into three generic groups: batch, mixed flow-through and column experiments. These three generic types of experiments are examined below. The net change in Si concentration with time as a result of plagioclase dissolution and kaolinite precipitation (Eq. 1) in a batch reactor may be described by:

$$\frac{dC}{dt} = 1.54 \cdot \text{Rate} \cdot \frac{m \cdot S}{V} \tag{2}$$

where, C is the concentration of Si (M), t is time (s), Rate is the net rate of the dissolution/precipitation reaction (Eq. 1) (mol m^{-2} s^{-1}), m is the plagioclase mass (g), S is the specific surface area of the plagioclase (m^2 g^{-1}) and V is the volume of the solution in the reactor (L). In a typical batch experiment 5 g of mineral are added to 0.1 l of solution and the change with time in solution concentration is measured. The rate is determined from a linear regression of the measured change in concentration with time. If the dissolution rate was 2×10^{-16} mol m^{-2} s^{-1} throughout the experiment, the expected daily increase in Si concentration (Eq. 2) would be 1.3×10^{-9} M. After 100 days of reaction the concentration would increase by 1.3×10^{-7} M, which is a change of less than 0.1% of the initial concentrations, i.e., much less than the analytical uncertainty in the determination of the Si concentration. The change in concentration with time may be enhanced by increasing the mass to volume ratio (m/V in Eq. 2). Indeed, increasing the m/V ratio to 1,000 g l^{-1}, would increase the release rate, yet the change in Si concentration after 100 days (2.7 μM = 1.4%) would not be significant within analytical uncertainty. It is important to emphasize that there is no problem in measuring concentrations of a few μM of Si. The problem is in observing an increase from 189 to 192 μM Si. Significantly increasing the m/V ratio above 1,000 g l^{-1} is not practical as it will be impossible to stir and to sample the solution. One may

suggest grinding the mineral in order to increase the specific surface area (S in Eq. 2), however by doing that, fresh surfaces would be formed replacing the highly weathered natural surfaces of the sample, and as a result the dissolution rate would be much faster than that observed in nature. Providing that the experimental conditions would be maintained constant throughout the experiment, at least 200 days are required in order to achieve the first data point that would be usable to estimate the rate, and almost 2 years to get two more points, which are required to estimate the rate using a linear regression. Because maintaining such an experiment under constant conditions for such a long time is not practical, it is therefore not possible to measure the slow dissolution rates observed in the Panola regolith using a standard batch experiment.

The differences between the input and the output concentrations in a mixed flow-through experiment at steady state may be calculated from the expression:

$$(C_{\text{out}} - C_{\text{inp}}) = 1.54 \cdot \text{Rate}\frac{m \cdot S}{q} \tag{3}$$

where C_{inp} and C_{out} are Si concentrations in the input and the output solutions, respectively (mol l^{-1}) and q is the fluid volume flux through the system (l s^{-1}). In a typical flow-through experiment, one inserts 5 g of mineral into a reactor, and a solution is pumped through it at a rate of 1×10^{-6} l s^{-1}. Under such conditions, the difference between the input and the output at steady state would be only 0.002 μM (0.001%). The difference in concentrations between the input and the output solution may be increased by increasing the mass to flow rate ratio (m/q in Eq. 3). Indeed, increasing m/q by a factor of 5,000 to 2.5×10^{10} g s l^{-1} would increase the difference between the output and the input concentrations to 8 μM (4%). However, in order not to increase the mineral mass/solution volume ratio above 1,000 g l^{-1}, the solution volume would have to be increased as well. As a result the residence time of the system (defined as V/q) would increase and it would take much longer to approach steady state. Figure 1 shows the predicted change in the output concentration of a flow-through experiment in which m/q is 2.5×10^{10} g s l^{-1} and m/V is 1,000 g l^{-1}. More than 2 years are required to approach steady state. Maintaining a flow-through experiment under constant conditions for such a long time is even more complicated than maintaining a batch experiment, and therefore it is not possible to measure the slow dissolution rates observed in the field using standard flow-through experiment.

To accurately relate the output solutions of a column dissolution experiment under near equilibrium conditions to the plagioclase dissolution rates (including variations of the rate due to changes in the degree of saturation along the column), either inverse theory or a forward model must be used (Mogollon et al. 1996). To simplify the calculations, we assume that the small changes in concentrations along the column do not significantly influence the dissolution rate, and therefore that it is constant along the column. In such a case the differences between the input and the output concentrations in the column experiment at steady state may be calculated using Eq. 3. The mineral mass to solution volume ratio in a column experiment is determined by the density and the porosity of the sample. Taking a reasonable porosity of 30% and oligoclase density of 2.65 kg l^{-1}, m/V would be 1,260 g l^{-1}. Therefore, the residence time in the column experiment would be shorter by 26% than that in a mixed flow-through experiment with m/V of 1,000 g l^{-1}. Yet, more than 1.5 years would be required to approach a steady state in a column experiment in which m/q is 2.5×10^{10} g s l^{-1}.

It is important to note that in the above discussion we took into account only the analytical uncertainty of the determination of the Si concentration. The actual evaluation of the dissolution rates involves other uncertainties in parameters that have been assumed to be constant throughout the experiment (e.g., the reactive surface area of the plagioclase). The simultaneous dissolution of plagioclase and precipitation of

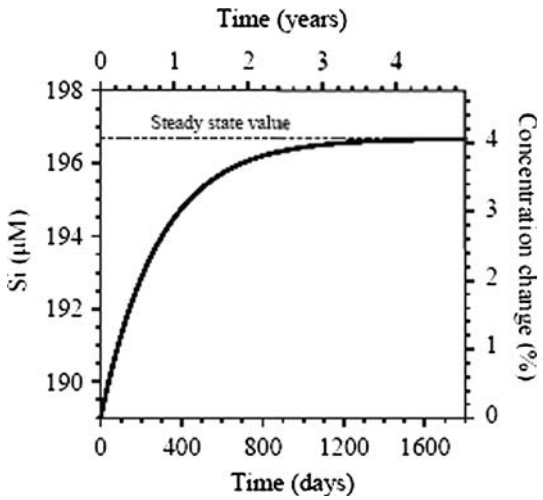

Fig. 1 Calculation of the expected change with time of the output concentration of a flow-through dissolution experiment of oligoclase with specific surface area of 1 m^2 g^{-1} in Panola pore water (Table 1). The mass to flow rate ratio (m/q) is 2.5×10^{10} g s l^{-1}, and the mass to volume ratio (m/V) is 1,000 g l^{-1}

secondary minerals (kaolinite in the present study calculations) adds more uncertainty to the interpretation of experiments simulating typical field conditions.

The extrapolation of laboratory dissolution rates to field conditions

As it is not possible to measure the dissolution rates under typical field conditions, dissolution rates have been determined under a variety of experimental conditions (See Blum and Stillings 1995; Brantley 2004 for review). The experimental conditions in each of these experiments differ in several aspects from the field conditions. The slowest laboratory dissolution rates of a plagioclase (1.3×10^{-15} mol m^{-2} s^{-1}) were obtained by White and Brantley (2003) after 6 years of dissolution of a weathered Panola Granite in a column experiments under far from equilibrium conditions. The pH in the column varied between 4.5 in the input and 5.5 at the output. This rate is six times faster than the rate of dissolution of the same plagioclase at pH 6.5 and under near equilibrium in the field (2×10^{-16} mol m^{-2} s^{-1}), as was estimated by White et al. (2001).

When all other environmental conditions held constant (e.g., organic ligands, pH, Fe (Hodson 2003), and Al (Oelkers et al. 1994) concentrations), the dependence of the overall dissolution and precipitation rates on the deviation from equilibrium may be described by:

$$\text{Rate} = k \cdot f(\Delta G_r) \tag{4}$$

where k is a coefficient that depends on the other environmental variables, and $f(\Delta G_r)$, accounts for the variation of the rate with the deviation from equilibrium. ΔG_r stands for the Gibbs free energy of the reaction. According to the transition state theory (TST), the dependence of the rate of an elementary reaction on the deviation from equilibrium [$f(\Delta G_r)$] is described by:

$$f(\Delta G_r) = 1 - \exp\left(\frac{\Delta G_r}{RT}\right) = 1 - 10^{\text{SI}} \tag{5}$$

where R is the gas constant and T is the temperature in Kelvin (Lasaga 1998), and SI is the saturation index. The function $f(\Delta G_r)$ for overall reactions is difficult to predict a priori. In many studies Eq. 5 is generalized to:

$$f(\Delta G_r) = 1 - \exp\left(\frac{n \cdot \Delta G_r}{RT}\right) = 1 - 10^{(n \cdot \text{SI})} \tag{6}$$

where n is a coefficient that is not necessarily equal to one (Lasaga 1998). The BCF (Burton Cabrera and Frank) crystal growth theory (Burton et al. 1951) describes the spiral growth of a step that is initiated by a screw dislocation. This theory describes the attachment of molecules (adatoms) on the mineral surface, which is followed by surface diffusion towards the step. The rate dependence on deviation from equilibrium predicted by BCF theory is based on the balance between the attachment and detachment of the adatoms and it predicts $n = 2$ for spiral growth (or dissolution) along steps that are initiated from a screw dislocation (Lasaga 1998). Equations 4, 5, 6 describe the effect of deviation from equilibrium on dissolution rate under conditions in which a single mechanism is dominant throughout the entire range of ΔG_r. However, there is a major change in the dominant reaction mechanism between the near-equilibrium and the far-from-equilibrium regions. This change in mechanism was attributed to the opening of etch pits once the solution is sufficiently undersaturated (Lasaga and Blum 1986; Burch et al. 1993; Beig and Luttge 2006). Therefore, in order to describe the effect of deviation from equilibrium on dissolution rates, the rate law should include the contribution of the dissolution of both the etch pits and the bulk mineral surface. Assuming that the dissolutions at these two sites are independent of each other, the overall dissolution rate will be the sum of the rates of the two mechanisms.

The effect of deviation from equilibrium on the albite dissolution rate was studied by Burch et al. (1993) at 80°C, pH 8.8 using a freshly ground Amelia albite and was found to be:

$$R_{\text{diss}} = -k_1\left[1 - e^{\left(8.4 \times 10^{-17} \cdot (\Delta G/RT)^{15}\right)}\right] - k_2\left[1 - e^{(\Delta G/RT)}\right]^{1.45} \tag{7}$$

where k_1 and k_2 are rate coefficients that depend on the environmental conditions. In contrast to the rate law of Eq. 5, this rate law is an empirical rate law, which is not based on kinetic theory. Nevertheless, the first term in Eq. 7 may be related to the dissolution of the etch pits and the second term to the dissolution of the non-etched surfaces of the albite. Feldspar dissolution rate is pH independent under circum neutral pH (Blum and Stillings 1995), and therefore the far from equilibrium dissolution rate of the plagioclase in the column experiments with the weathered Panola Granite of White and Brantley (2003) (1.3×10^{-15} mol m^{-2} s^{-1}) is a reasonable proxy for the value of k_1 at ambient temperature and pH 6.5. Assuming that the ratio between the rate coefficient of the bulk plagioclase and

that of the etch pits (k_2/k_1) is the same in albite and oligoclase and is independent of temperature and pH, the value of k_2 at 25°C and pH 6.5 may be calculated from the product of k_1 under these conditions and the ratio of k_2/k_1, which was determined for albite at 80°C and pH 8.8 (0.0896 Burch et al. 1993) to be 1.2×10^{-16} mol m^{-2} s^{-1}. Further assuming that the same $f(\Delta G_r)$ function governs the dissolution rate of albite at 80°C and pH 8.8 and the rate of oligoclase at ambient temperature and pH 6.5, the dissolution of the plagioclase in the Panola granite may be simulated using the equation:

$$\begin{aligned} R_{\text{diss}} &= -1.3 \times 10^{-15} \cdot \left[1 - e^{\left(8.4 \times 10^{-17} \cdot (\Delta G/RT)^{15}\right)}\right] \\ &\quad - 1.2 \times 10^{-16} \left[1 - e^{(\Delta G/RT)}\right]^{1.45} \\ &= -1.3 \times 10^{-15} \cdot \left(1 - 10^{\left(8.4 \times 10^{-17} \cdot \text{SI}^{15}\right)}\right) \\ &\quad - 1.2 \times 10^{-16} (1 - 10^{\text{SI}})^{1.45} \end{aligned} \tag{8}$$

If the effects of all the other parameters on dissolution rate are relatively small, the prediction of the laboratory experiments for the dissolution rate of the Panola Granite in the field may be represented by Eq. 8. As will be shown below, the field based estimation of plagioclase dissolution rates are much faster than the prediction of Eq. 8.

In the following simulation, the change in concentrations of Al, Si, Na and Ca, as well as the change in the expected dissolution rate of plagioclase in a regolith of the Panola granite was calculated using the following simple assumptions: (1) the pH of the solution is constant and equal to 6.5; (2) the only phase that is dissolved is the plagioclase ($Na_{0.77}Ca_{0.23}Al_{1.23}Si_{2.77}O_8$); (3) secondary phases are not precipitating; and (4) the dissolution rate of the plagioclase is solely determined by the rate law of Eq. 8. We started with some nominal small concentrations of Na, Ca, Si, Al, and an oligoclase to water ratio of 150 g/l. We used a BET surface area of 0.13 m^2/g. The standard Gibbs free energy for oligoclase dissolution reaction (Eq. 1) was calculated using the method of Arnorsson and Stefansson (1999). The resulting log K for the oligoclase dissolution is –17.74. All equilibrium constants for aqueous complexes are from (Nordstrom et al. 1990).

The calculated changes in concentrations of Al, Si, Na and Ca as a function of time are shown in Fig. 2. After a short period (20 years) of a very steep increase in cation concentrations, a less steep and almost constant increase of concentrations is observed. As solutes further accumulate, the aqueous solution approaches equilibrium with respect to oligoclase (Fig. 3). The change in oligoclase dissolution rate with time reveals two distinct plateaus (Fig. 4). The first rate plateau with a rate of 1.42×10^{-15} mol m^{-2}s^{-1} appears in the initial period of the simulation (the first 12 years) during which the first term of Eq. 8 dominates the oligoclase dissolution. At this stage, the solution is highly undersaturated with respect to oligoclase, and the saturation indices of the oligoclase ranges from –6 to –10. The second rate plateau with a rate of 1.2×10^{-16} mol m^{-2}s^{-1} appears after about 160 years as the second term in Eq. 8 dominates the rates. After about 1,200 years, as the saturation indices becomes higher than –1 (Fig. 3), the dissolution rate of oligoclase significantly decreases. As the solution approaches saturation with respect to oligoclase, the dissolution rate approaches zero (Fig. 5); after 6,000 years the rate is 10^{-18} mol m^{-2} s^{-1}, i.e., more than two orders of magnitude slower than field estimation of oligoclase dissolution rates (2×10^{-16} mol m^{-2} s^{-1} [White and Brantley 2003]).

In contrast to the common view that laboratory experiments predict dissolution rates which are faster than that in the field, the simulation which was based on the combination of the far from equilibrium experiments of White and Brantley (2003) and the effect of deviation from equilibrium of Burch et al. (1993) indicates that laboratory dissolution experiments actually predict slower rates than those observed in the field. Changing the parameters in Eq. 8 or using different forms of $f(\Delta G_r)$ does not change the major outcome of the simulation—the solution approaches

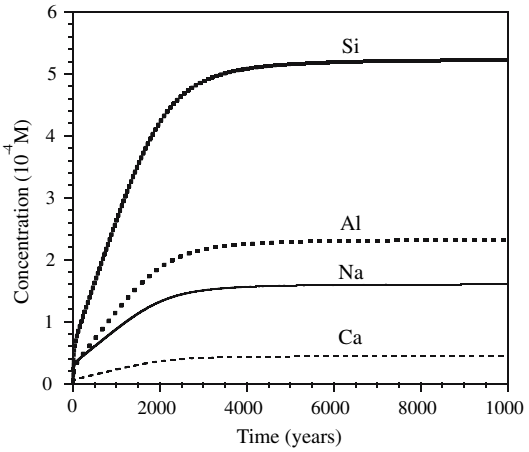

Fig. 2 The calculated change in Ca, Na, Si and Al concentrations with time during the course of a simulation of oligoclase dissolution with a specific surface area of 0.13 m^2 g^{-1} and a mass to volume ratio (m/V) of 150 g l^{-1}. The dissolution rate is controlled by the rate law of Eq. 8. Secondary phases are not allowed to precipitate in this simulation

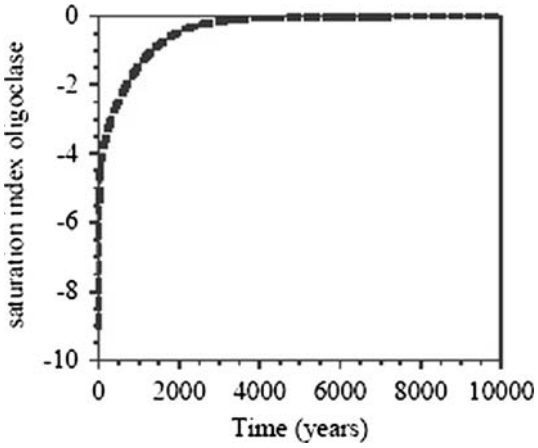

Fig. 3 The calculated change in saturation index of oligoclase with time during the course of a simulation of oligoclase dissolution in which secondary phases are not allowed to precipitate. The parameters of the simulation are described in the caption of Fig. 2

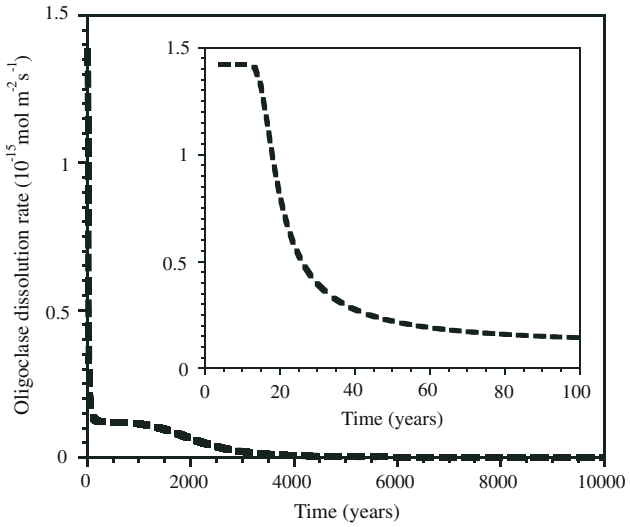

Fig. 4 The calculated change in dissolution rate of oligoclase with time during the course of a simulation of oligoclase dissolution in which secondary phases are not allowed to precipitate. The parameters of the simulation are described in the caption of Fig. 2. Enlargement of the first 100 h is shown in the insert

equilibrium with respect to the plagioclase after a relatively short period of time, and consequently the dissolution rate approaches zero.

Many field studies indicate that, in contrast to the above simulation, the dissolution rate does not approach zero even after a very long flow path (Zhu et al. 2004; Zhu 2005). In the above simulation, in contrast to actual field observations, we assume that secondary phases are not precipitating. The effect of the precipitation of secondary minerals on the dissolution of the primary minerals is therefore examined in the following section.

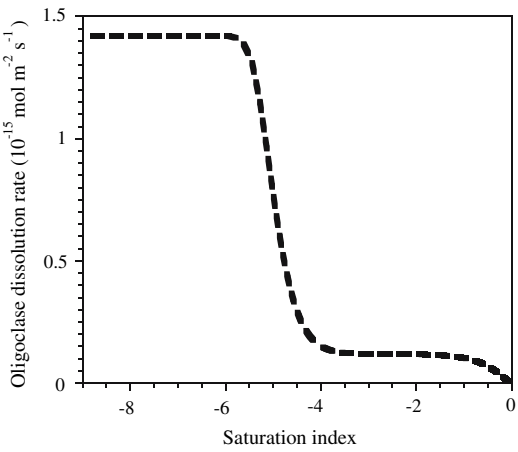

Fig. 5 The effect of saturation on oligoclase dissolution rate according to the rate law of Eq. 8

The effect of secondary mineral precipitation on the dissolution of primary minerals

In this section, we simulated the change in concentration during oligoclase dissolution and kaolinite precipitation. An experimental $f(\Delta G)$ function for the dissolution of kaolinite at 80°C and pH 3 was derived by Nagy et al. (1991) to be:

$$f(\Delta G_r) = 1 - e^{(\Delta G_r/RT)^{0.9 \pm 0.2}} \quad (9)$$

Within error, this rate law is identical to the prediction of transition state theory (Eq. 5). By applying the principle of detailed balancing, one can multiply the $f(\Delta G_r)$ of Eq. 5 by the far from equilibrium dissolution rate of kaolinite, to predict the dependence of the precipitation rate of kaolinite on deviation from equilibrium. This method was recently verified for quartz dissolution and precipitation at 180°C and pH 4 (Ganor et al. 2005). However, to do that one needs to know the far from equilibrium dissolution rate of kaolinite under field conditions.

The far from equilibrium dissolution rate of kaolinite at 25°C and pH around 6.5 was determined in laboratory experiments by Wieland and Stumm (1992) to be $10^{-12.6}$ mol m^{-2} s^{-1} and by Carroll and Walther (1990) to be 10^{-13} mol m^{-2} s^{-1}. It is reasonable to assume that similarly to the oligoclase, the reactivity of kaolinite in the field is a few orders of magnitude lower than that of the fresh kaolinite, which was used in the experiments of Wieland and Stumm (1992) and Carroll and Walther (1990). Therefore, one cannot simply

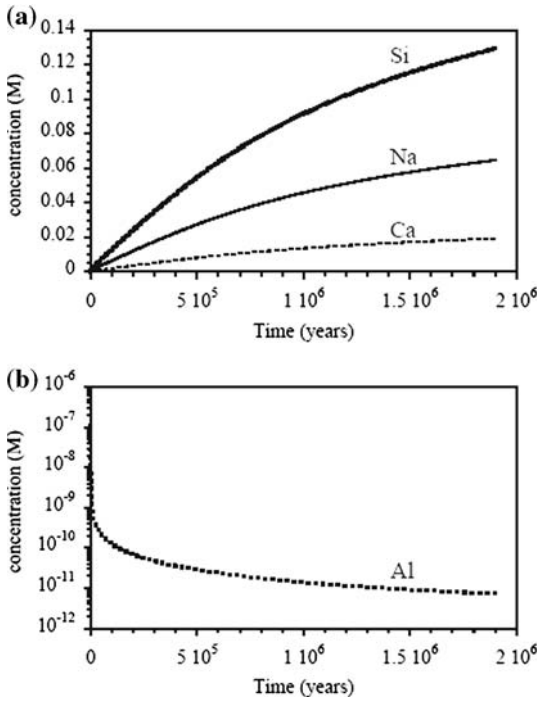

Fig. 6 The calculated change in Ca, Na, and Si concentrations (**a**), and Al concentration (**b**) with time during the course of a simulation of oligoclase dissolution and kaolinite precipitation. The specific surface area of the oligoclase is 0.13 $m^2\ g^{-1}$ and its mass to volume ratio (m/V) is 150 g l^{-1}. The dissolution rate of the oligoclase dissolution is controlled by the rate law of Eq. 8 and the rate of the kaolinite precipitation by the rate laws of Eqs. 4 and 5. The effective rate coefficient of kaolinite precipitation was set to be 3.7×10^{-18} mol $l^{-1}\ s^{-1}$

adopt the laboratory rates for the simulation. Another source of uncertainty is related to the estimation of the amount of kaolinite in the regolith and its surface area. To circumvent these uncertainties, we described the kaolinite dissolution/precipitation rate using an effective rate coefficient (mol $l^{-1}\ s^{-1}$), which represents the product of the rate constant of kaolinite dissolution (mol $m^{-2}\ s^{-1}$), the specific surface area of the kaolinite ($m^2\ g^{-1}$ kaolinite) and the kaolinite/water ratio (g l^{-1}). The effect of the magnitude of this effective rate coefficient on the simulation is discussed later on in the paper.

In the simulations below, we used the rate laws of Eqs. 8 and 5 to describe the effect of deviation from equilibrium on oligoclase dissolution and kaolinite precipitation, respectively. We substitute the coefficient k in Eq. 4 by an effective rate coefficient of 3.7×10^{-18} mol $l^{-1}\ s^{-1}$. As shown below, the general behavior of the simulation was not significantly influenced by picking other values of the rate coefficient in the range of 10^{-14} to 10^{-19} mol $m^{-2}\ s^{-1}$. The other parameters of the simulations were identical to the parameters that were used in the previous simulation.

The calculated changes in concentrations of Al, Si, Na, and Ca with time are shown in Fig. 6a and b. The concentrations of Si, Na and Ca increase but do not reach a constant value even after almost two million years. In contrast, Al concentration decreases to values which are below the detection limits of available analytical methods. These trends differ from those obtained without kaolinite precipitation (cf., Fig. 2). The changes with time in oligoclase dissolution and kaolinite precipitation rates are shown in Fig. 7. To simplify the comparison, both rates are presented in units of mol $l^{-1}\ s^{-1}$. During the first 200 years of the simulation, the dissolution rate of oligoclase is constant and is controlled by the first term of Eq. 8. At this stage, the solution is highly undersaturated with respect to oligoclase, and the saturation index of the oligoclase changes from –13 to –6 (Fig. 8a). During this period, the saturation index of the kaolinite is constant (Fig. 8b), and as a result the precipitation rate of kaolinite is also constant (Fig. 7b). A second rate plateau appears after about 10,000 years of simulation in which the rates of oligoclase dissolution and kaolinite precipitation dropped by more than one order of magnitude. During the next few hundreds of thousands of years, the second term in Eq. 8 dominates the oligoclase dissolution rates, which remain about constant as the saturation index with respect to oligoclase ranges between –4 and –1.2. At the same time, the saturation index with respect to kaolinite is almost constant (Fig. 8b), and as a result the precipitation rate of kaolinite is also almost constant (Fig. 7b). After about 400,000 years, as the saturation index of oligoclase becomes higher than –1 and that of kaolinite lower than 2.5 (Fig. 8b), the rates of oligoclase dissolution and kaolinite precipitation start to decrease faster. The final calculated dissolution rate of oligoclase after almost two million years of simulation is 3.2×10^{-17} mol $m^{-2}\ s^{-1}$ (6.3×10^{-16} mol $l^{-1}\ s^{-1}$), which is almost three orders of magnitude faster than that after 10,000 years of simulation without kaolinite.

At each step of the simulation, the dissolution rate of the oligoclase and the precipitation rate of the kaolinite are independently determined by their saturation indices via Eqs. 8 and 5, respectively (Fig. 9). As the two saturation indices depend on the activities of Al and Si in solution, it is expected that the two rates would be somewhat correlated. The striking result of the simulation is that the two rates are completely coupled (Fig. 10). After less than 100 years of simulation, the ratio between the dissolution rate of the oligoclase and the precipitation rate of the kaolinite is stabilized on a value of 1.626. In the following section we will show that regardless of the mechanisms and

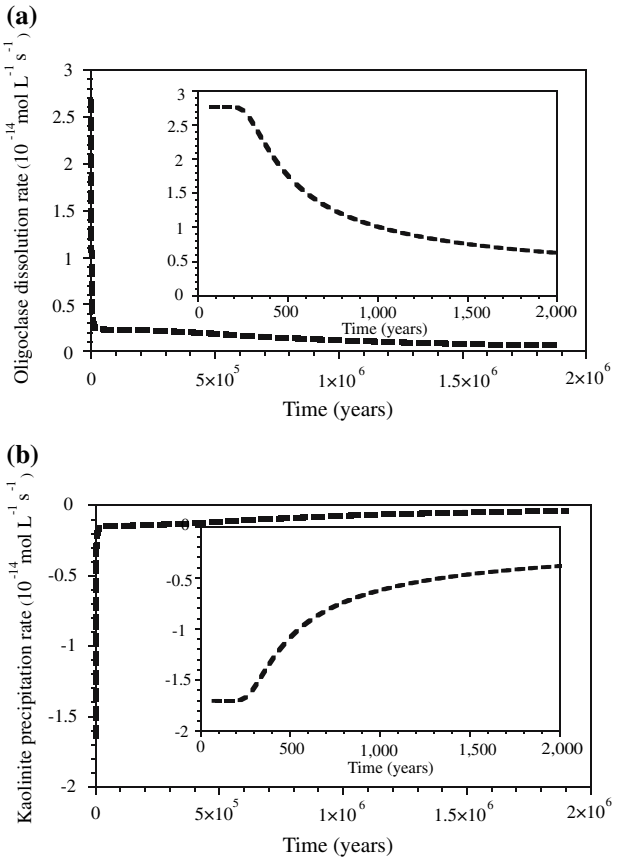

Fig. 7 The calculated change in the dissolution rate of oligoclase (**a**) and precipitation rate of kaolinite (**b**) with time during the course of a simulation of oligoclase dissolution and kaolinite precipitation. Enlargements of the first 2,000 h are shown in the inserts of (**a**) and (**b**). The parameters of the simulation are described in the caption of Fig. 6

rate laws that govern the dissolution and precipitation of the two minerals, their stoichiometry dictates the observed rate ratio of 1.626.

The stoichiometry of the overall dissolution/precipitation reaction may be described by the general equation:

$$\begin{aligned} &X\ Na_{0.77}Ca_{0.23}Al_{1.23}Si_{2.77}O_8 + (4.92X - 6Y)H^+ \\ &\quad + (3.08X + Y)\ H_2O \rightarrow Y\ Al_2Si_2O_5(OH)_4 \\ &\quad + (2.77X - 2Y)\ H_4SiO_4 + (1.23X - 2Y)\ Al^{3+} \\ &\quad + 0.23X\ Ca^{2+} + 0.77X\ Na^+ \end{aligned} \quad (10)$$

If the instantaneous rates of the oligoclase dissolution and the kaolinite precipitation (in units of mol l^{-1} s^{-1}) are X, and Y respectively, the change in Al concentration with time will be $1.23X - 2Y$. For the observed rate ratio ($X/Y = 1.626$), the change with time in Al concentration is zero. In other words, for this rate ratio the stoichiometry of the overall dissolution/precipitation reaction is that of Eq. 1. For lower rate ratio the Al concentration would decrease with time, whereas for higher ratios, the Al concentration would increase with time. As the Al concentration approaches zero, its concentration cannot decrease anymore, and therefore the rate ratio cannot be lower than 1.626. The increase of the rate ratio is limited too, due to a feedback between this rate ratio and the saturation indexes of oligoclase and kaolinite: any increase in the rate ratio (due to either an increase in the oligoclase dissolution rate or a decrease in the kaolinite precipitation rate) would decrease the undersaturation with respect to oligoclase dissolution and increase the oversaturation with respect to kaolinite. As a result, the dissolution rate of oligoclase would decrease, the precipitation rate of kaolinite would increase, and the rate ratio would decrease back towards 1.626. Due to this negative feedback, the rate ratio cannot increase to a higher value. The ratio of 1.626 is determined by the stoichiometry coefficients of Al in the kaolinite and oligoclase (Eq. 10). Changing the stoichiometry coefficients of Al in the primary and the secondary minerals in the simulations would change this rate ratio. In general, the ratio between the rate of dissolution of the primary mineral and the rate of precipitation of the secondary mineral would approach the ratio between the stoichiometry coefficients of Al in the secondary mineral and that of Al in the primary mineral.

Figure 11 compares the change with time in oligoclase dissolution rate in simulation with different effective rate coefficients of kaolinite precipitation. The changes in oligoclase dissolution rate in the simulations are bounded between two end member scenarios: one in which kaolinite precipitation rate is very fast and as a result the solution is forced to be in equilibrium with the kaolinite, and the second in which precipitation rate is zero (i.e., kaolinite does not precipitate). With the exception of the simulation in which the kaolinite precipitation rate was set to be zero, the different simulations show similar trends. Regardless of the effective rate coefficients of kaolinite precipitation, the above mentioned two rate plateaus were observed in all the simulations. In addition, the oligoclase dissolution/kaolinite precipitation rate ratio approaches 1.626 in all these simulations.

The effective precipitation rate of kaolinite controls the change in the saturation index with time. For a faster effective precipitation rate of kaolinite, the degree of under-saturation with respect to oligoclase dissolution is higher and the degree of over-saturation with respect to kaolinite precipitation is slower. As a result, the rate of oligoclase dissolution is faster when the effective precipitation rate of kaolinite is faster.

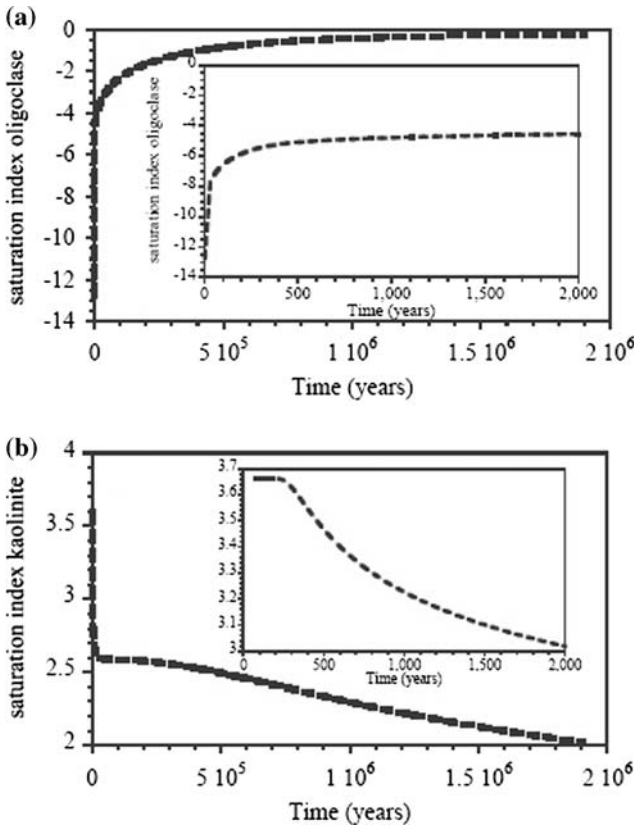

Fig. 8 The calculated change in the saturation index of oligoclase (**a**) and kaolinite (**b**) with time during the course of a simulation of oligoclase dissolution and kaolinite precipitation. Enlargements of the first 2,000 h are shown in the inserts of (**a**) and (**b**). The parameters of the simulation are described in the caption of Fig. 6

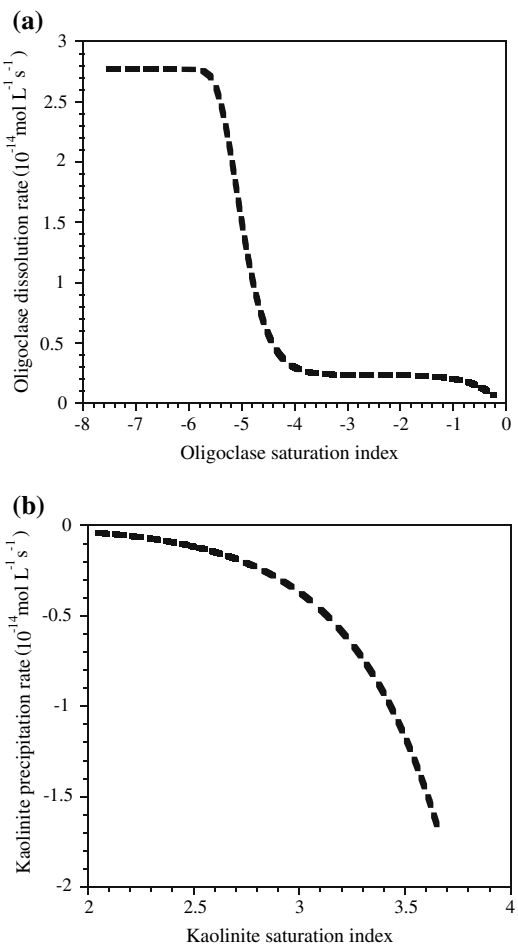

Fig. 9 The calculated change in the dissolution rate of oligoclase (**a**) and precipitation rate of kaolinite (**b**) with their saturation indices. The parameters of the calculations are described in the caption of Fig. 6

Summary and conclusions

Much of the long-standing discussion of the discrepancy between field and laboratory dissolution rates focused on the actual differences between the two settings, and paid not enough attention to the differences in the methods that are used to determine the rates. The present study shows that the slow rates of mineral dissolution that are observed in the field cannot be determined using standard laboratory methods. It is therefore not surprising that there is a discrepancy between field-base dissolution rates and laboratory experiments.

The environmental conditions in the field are more complicated in many aspects than the simple simulation presented above. For example, both the reactivities of the minerals and their amounts were kept constant in the simulation although they vary in the field as a function of time. Our simulation therefore cannot be used to predict the change with time of dissolution rate in the field as a result of these factors. However, there are several aspects of the simulations

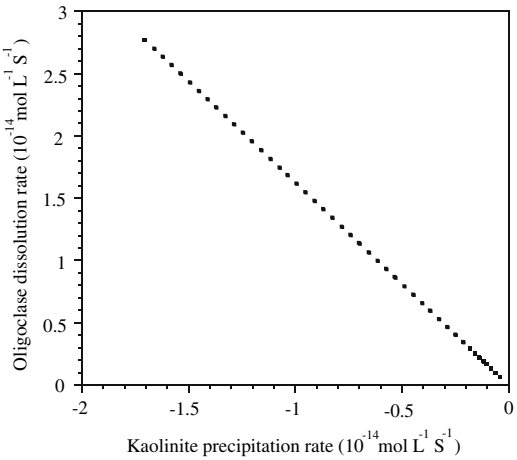

Fig. 10 The coupling between oligoclase dissolution and kaolinite precipitation in the simulation. The parameters of the calculations are described in the caption of Fig. 6

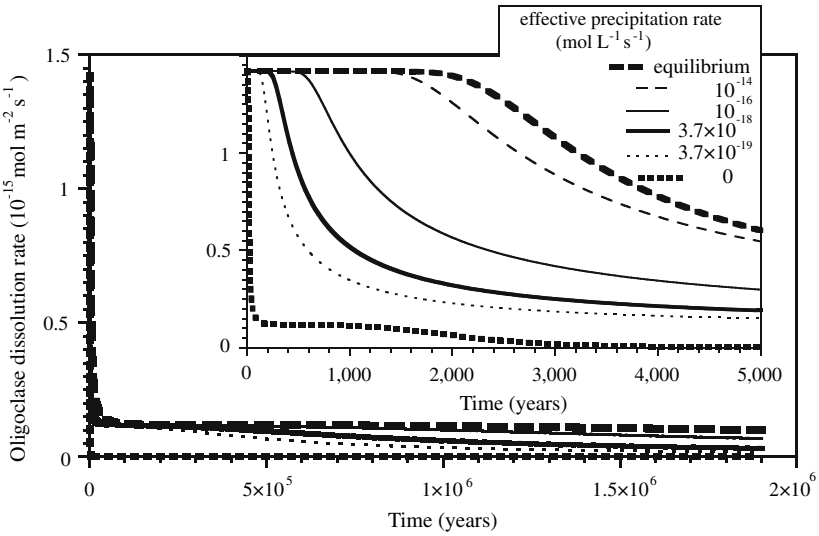

Fig. 11 Comparison of the change with time of oligoclase dissolution rate in simulations with different effective rate coefficients of kaolinite precipitation. Enlargement of the first 5,000 h of the simulations is shown in the insert

that may be used to understand the dissolution rates in the field. Regardless of the reactivity of the plagioclase and the rate of the dissolution reaction, the simulations demonstrate that without precipitation of secondary minerals the dissolution rate of plagioclase would be halted. Moreover, the change with time of the dissolution rate depends on the rate of the precipitation. We suggest that the coupling between the dissolution and the precipitation that was observed in the simulation must exist in the field. Taking into account that the concentration of Al in the field is close to zero, the ratio between the rates (in units of m/s) of the plagioclase dissolution and the precipitation of the secondary minerals should equal the ratio between the stoichiometry coefficients of Al in the secondary mineral and that of Al in the plagioclase. Any attempt to predict the dissolution rate in the field requires the knowledge of the effective rate of the secondary mineral precipitation, which is as important as the rate of dissolution of the plagioclase. Therefore, the lack of data on precipitation rates of secondary minerals put a major constraint on our ability to accurately simulate the dissolution rate of plagioclase in the field.

Our simulation showed a decrease with time in the degree of undersaturation with respect to plagioclase dissolution, and a consequent decrease in its dissolution rate. Previous studies showed that the dissolution rate in the field indeed decreases as a function of soil age (e.g., Taylor and Blum 1995) and flow paths (Zhu 2005). This decrease in rate with time was mostly related to changes in intrinsic properties such as the decrease in the reactivity of the mineral surfaces with time. In the present study, we show that part of the change with time in dissolution rate may be attributed to changes with time in the degree of undersaturation. It is important to note that the changes in the degree of saturation of the solution is measured using a different clock than that for the intrinsic properties of the primary minerals. The changes in the degree of saturation are related to the time that the solution was exposed to the minerals. In contrast, the changes in the reactivity of the mineral surface are related to the integrated time that the mineral was exposed to the solution, which may be approximated from the age of the soil. As the system is open, the age of the water may be much younger than that of the soil.

Acknowledgments This research is supported by the US Department of Energy (DE-FG26-04NT42125) and by National Science Foundation grants (EAR0423971 and EAR0509775) awarded to CZ. However, the views and opinions of authors expressed herein do not necessarily state or reflect those of the United States Government or any agency thereof.

References

Anbeek C (1993) The effect of natural weathering on dissolution rates. Geochim Cosmochim Acta 57:4963–4975

Arnorsson S, Stefansson A (1999) Assessment of feldspar solubility constants in water in the range 0 to 350°C at vapor saturation pressures. Amer J Sci 299:173–209

Beig MS, Luttge A (2006) Albite dissolution kinetics as a function of distance from equilibrium: implications for natural feldspar weathering (in press). Geochim Cosmochim Acta

Berner RA (1992) Weathering, plants and the long term carbon cycle. Geochim Cosmochim Acta 56:3225–3231

Blum A, Stillings LL (1995) Feldspar dissolution kinetics. In: White AF, Brantley SL (eds) Chemical weathering rates of silicate minerals, vol 31. Mineralogical Society of America, USA, pp 291–351

Brantley SL (2004) Reaction kinetics of primary rock-forming minerals under ambient conditions. In: Holland HD, Turekian KK (eds) Treatise on Geochemistry. Elsevier, Newyork

Bricker OP, Jones B, Bowser CJ (2004) Mass-balance approach to interpreting weathering reactions in watershed systems. In: Surface and ground water, weathering, and soils, vol 5. Elsevier Science, pp 119–132

Burch TE, Nagy KL, Lasaga AC (1993) Free energy dependence of albite dissolution kinetics at 80°C, pH 8.8. Chem Geol 105:137–162

Burton WK, Cabrera N, Frank FC (1951) The growth of crystals and the equilibrium structure of their surfaces. Philos Trans R Soc Lond 243:299–358

Carroll SA, Walther JV (1990) Kaolinite dissolution at 25°, 60°, and 80°C. Amer J Sci 290:797–810

Casey WH, Banfield JF, Westrich HR, McLaughlin L (1993) What do dissolution experiments tell us about natural weathering? Chem Geol 105:1–15

Drever JI (2003) Surface and ground water, weathering, and soils. In: Holland HD, Turekian KK (eds) Treatise on Geochemistry, vol 5. Elsevier Science, pp 626

Ganor J, Huston TJ, Walter LM (2005) Quartz precipitation kinetics at 180°C in NaCl solutions—implications for the usability of the principle of detailed balancing. Geochim Cosmochim Acta 69(8):2043–2056

Huntington TG, Hooper RP, Johnson CE, Aulenbach BT, Cappellato R, Blum AE (2000) Calcium depletion in forest ecosystems of southeastern United States. Soil Sci Soc Amer J 64:1845–1858

Lasaga AC (1998) Kinetic theory in the earth sciences. Princeton University Press, Newyork

Lasaga AC, Blum AE (1986) Surface chemistry, etch pits and mineral-water reactions. Geochim Cosmochim Acta 50:2363–2379

Lasaga AC, Soler JM, Ganor J, Burch TE, Nagy KL (1994) Chemical weathering rate laws and global geochemical cycles. Geochim Cosmochim Acta 58(10):2361–2386

Mogollon JL, Ganor J, Soler JM, Lasaga AC (1996) Column experiments and the full dissolution rate law of gibbsite. Amer J Sci 296:729–765

Nagy KL, Blum AE, Lasaga AC (1991) Dissolution and precipitation kinetics of kaolinite at 80°C and pH 3: the dependence on solution saturation state. Amer J Sci 291:649–686

Nordstrom DK, Plummer LN, Langmuir D, Busenberg E, May HM, Jones B, Parkhurst DL (1990) Revised chemical equilibrium data for major water-mineral reactions and their limitations. In: Melchior DC, Bassett RL (eds) Chemical modeling of aqueous systems II. American Chemical Society, pp 398–413

Hodson ME (2003) The influence of Fe-rich coatings on the dissolution of anorthite a pH 2.6. Geochim Cosmochim Acta 67(18):3355–3363

Oelkers EH, Schott J, Devidal JL (1994) The effect of aluminum, pH, and chemical affinity on the rates of aluminosilicate dissolution reactions. Geochim Cosmochim Acta 58:2011–2024

Schnoor JL (1990) Kinetics of chemical weathering: a comparison of laboratory and field weathering rates. In: Stumm (ed) Aquatic chemical kinetics: reaction rates of processes in natural waters. Wiley, pp 475–504

Stumm W (1992) Chemistry of the solid–water interface: processes at the mineral–water and particle–water interface in natural systems. Wiley, Newyork

Taylor A, Blum JD (1995) Relation between soil age and silicate weathering rates determined from the chemical evolution of a glacial chronosequence. Geology 23(11):979–982

van Grinsven HJM, van Riemsdijk WH (1992) Evaluation of batch and column techniques to measure weathering rates in soils. Geoderma 52(1–2):41–57

Velbel MA (1993) Constancy of silicate-mineral weathering-rate ratios between natural and experimental weathering: implications for hydrologic control of differences in absolute rates. Chem Geol 105:89–99

White AF, Blum AE, Schulz MS, Huntington TG, Peters NE, Stonestrom DA (2002) Chemical weathering of the Panola Granite: solute and regolith elemental fluxes and the dissolution rate of biotite. In: Hellmann R, Wood SA (eds) Water–rock interaction, ore deposits, and environmental geochemistry: a tribute to David A. Crerar. The Geochemical Society, Special Publication No. 7 pp 37–59

White AF, Brantley SL (1995) Chemical weathering rates of silicate minerals. In: Ribbe PH (ed) Reviews in mineralogy, vol 31. Mineralogical Society of America, pp 583

White AF, Brantley SL (2003) The effect of time on the weathering of silicate minerals: why do weathering rates differ in the laboratory and field? Chem Geol 202:479–506

White AF, Bullen TD, Schulz MS, Blum AE, Huntington TG, Peters NE (2001) Differential rates of feldspar weathering in granitic regoliths. Geochim Cosmochim Acta 65:847–869

Wieland E, Stumm W (1992) Dissolution kinetics of kaolinite in acidic aqueous solutions at 25°C. Geochim Cosmochim Acta 56:3339–3355

Zhu C (2005) In situ feldspar dissolution rates in an aquifer. Geochim Cosmochim Acta 69(6):1435–1453

Zhu C, Blum A, Veblen D (2004) Feldspar dissolution rates and clay precipitation in the Navajo aquifer at Black Mesa, Arizona, USA. In: Eleventh international symposium on water–rock interaction WRI-11, pp 895–899